

## A new slant on hadron structure

W DETMOLD, D B LEINWEBER, W MELNITCHOUK<sup>1</sup>, A W THOMAS and  
S V WRIGHT

Department of Physics, and Mathematical Physics and Special Research Centre for the Subatomic  
Structure of Matter, Adelaide University, Adelaide SA 5005, Australia

<sup>1</sup> Also at Jefferson Lab., 12000 Jefferson Ave., Newport News, VA 23606, USA

Email: athomas@physics.adelaide.edu.au

**Abstract.** Rather than regarding the restriction of current lattice QCD simulations to quark masses that are 5–10 times larger than those observed as a problem, we note that this presents a wonderful opportunity to deepen our understanding of QCD. Just as it has been possible to learn a great deal about QCD by treating  $N_c$  as a variable, so the study of hadron properties as a function of quark mass is leading us to a deeper appreciation of hadron structure. As examples we cite progress in using the chiral properties of QCD to connect hadron masses, magnetic moments, charge radii and structure functions calculated at large quark masses within lattice QCD with the values observed physically.

**Keywords.** Hadron structure; lattice quantum chromodynamics.

**PACS Nos** 12.38.Gc; 11.15.Ha

### 1. Introduction

In striving to understand the properties of QCD the generalization to an arbitrary number of colours,  $N_c$ , particularly the limit  $N_c \rightarrow \infty$  (or ‘large  $N_c$ ’) has been extremely valuable. It has even proven possible to distinguish between models of hadron structure and to guide the further developments of such models on the basis of their large  $N_c$  behaviour [1]. Until recently it has generally been regarded as an unfortunate liability that current limitations on computer power restrict lattice QCD simulations with dynamical fermions to large quark masses. We would like to present a rather different view concerning the lattice data at large quark masses. In particular, we argue that like the behaviour as a function of  $N_c$ , lattice results as a function of quark mass offer extremely valuable new insights into the nature of QCD and especially into hadron structure.

To be a little more quantitative, the restriction to large quark masses in lattice simulations means typically 50 MeV or higher. Thus, in order to compare hadron properties calculated on the lattice one has to extrapolate as a function of quark mass (on top of all the other extrapolations, lattice spacing, lattice size, etc.) all the way to the physical light quark masses, around 5 or 6 MeV. Such extrapolations are complicated enormously by the fact that chiral symmetry is spontaneously broken in QCD. The mass of the pion, which is the Goldstone boson corresponding to this broken symmetry [2], behaves as:

$$m_\pi^2 \propto \bar{m}, \quad (\text{with } \bar{m} = m_u = m_d \neq 0), \quad (1)$$

as the quark mass,  $\bar{m}$ , moves away from zero – this is the Gell Mann–Oakes–Renner (GOR) relation. While eq. (1) is, in principle, only guaranteed for quark masses, near zero, explicit lattice calculations show that it holds over an enormous range, as high as  $m_\pi \sim 1$  GeV. For convenience, rather than measuring the deviation from exact chiral symmetry using  $\bar{m}$ , which is scale dependent, we shall use  $m_\pi^2$ .

In terms of  $m_\pi$ , current lattice calculations are typically restricted to pion masses larger than 500 MeV, with some pioneering work reporting preliminary results as low as 310 MeV. In order to compare these results with experimental data on hadron properties it is necessary to extrapolate the calculations at large pion masses to the physical value. In doing so it is crucial to respect the constraints imposed by chiral symmetry in QCD. In particular, as we discuss below, the existence of Goldstone bosons necessarily leads to behaviour which is *non-analytic* in the quark mass.

The structure of this article is that we first explain the origin of the non-analyticity associated with Goldstone boson loops. We then explain, using the specific case of the nucleon mass, how this non-analytic structure has been incorporated into a new method for extrapolating hadron masses from the large values characteristic of lattice calculations to the physical region. The consequences of this for the sigma commutator are then explained. Next we turn to recent results for baryon electromagnetic properties. Finally we discuss the most recent investigations of the proton structure function, especially the importance of chiral symmetry in connecting existing calculations of lattice moments with data. We conclude with a summary of the promised insights into the nature of hadron structure within QCD that follow from all these investigations.

## 2. Goldstone boson loops and non-analyticity

For our purposes the primary significance of spontaneous chiral symmetry breaking in QCD is that there are contributions to hadron properties from loops involving the resulting Goldstone bosons. These loops have the unique property that they give rise to terms in an expansion of most hadronic properties as a function of quark mass which are not analytic. As a simple example we consider the nucleon mass. The most important chiral corrections to  $M_N$  come from the processes  $N \rightarrow N\pi \rightarrow N$  ( $\sigma_{NN}$ ) and  $N \rightarrow \Delta\pi \rightarrow N$  ( $\sigma_{N\Delta}$ ). (We will come to what it means to say these are the most important shortly.) We write  $M_N = M_N^{\text{bare}} + \sigma_{NN} + \sigma_{N\Delta}$ . In the heavy baryon limit one has

$$\sigma_{NN} = -\frac{3g_A^2}{16\pi^2 f_\pi^2} \int_0^\infty dk \frac{k^4 u^2(k)}{k^2 + m_\pi^2}, \quad (2)$$

where  $g_A, f_\pi$  are strictly evaluated in the chiral limit. Here  $u(k)$  is a natural high momentum cut-off which is the Fourier transform of the source of the pion field (e.g. in the cloudy bag model (CBM) it is  $3j_1(kR)/kR$ , with  $R$  the bag radius [3]). From the point of view of PCAC it is natural to identify  $u(k)$  with the axial form factor of the nucleon, a dipole with mass parameter  $1.02 \pm 0.08$  GeV.

Regardless of the form chosen for the ultra-violet cut-off, one finds that  $\sigma_{NN}$  is a non-analytic function of the quark mass. The leading non-analytic (LNA) piece of  $\sigma_{NN}$  is independent of the form factor and gives

$$\sigma_{NN}^{\text{LNA}} = -\frac{3g_A^2}{32\pi f_\pi^2} m_\pi^3 \sim \bar{m}^{\frac{3}{2}}. \quad (3)$$

This has a branch point, as a function of  $\bar{m}$ , at  $\bar{m} = 0$ . Such terms can only arise from Goldstone boson loops.

### 2.1 Case study: The nucleon mass

It is natural to ask how significant this non-analytic behaviour is in practice. If the pion mass is given in GeV,  $\sigma_{NN}^{\text{LNA}} = -5.6m_\pi^3$  and at the physical pion mass it is just  $-17$  MeV. However, at only three times the physical pion mass,  $m_\pi = 420$  MeV, it is  $-460$  MeV – half the mass of the nucleon. If one’s aim is to extract physical nucleon properties from lattice QCD calculations this is extremely important. The most sophisticated lattice calculations with dynamical fermions are only just becoming feasible at such low masses and to connect to the physical world one must extrapolate from  $m_\pi \sim 500$  MeV to  $m_\pi = 140$  MeV. Clearly one must have control of the chiral behaviour.

Figure 1 shows recent lattice calculations of  $M_N$  as a function of  $m_\pi^2$  from CP-PACS and UKQCD [4]. The dashed line indicates a fit which naively respects the presence of a LNA term,

$$M_N = \alpha + \beta m_\pi^2 + \gamma m_\pi^3, \quad (4)$$

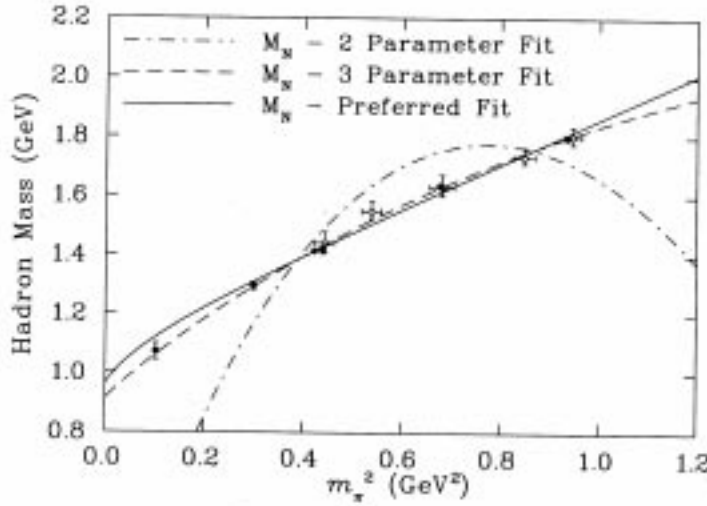


**Figure 1.** A comparison between phenomenological fitting functions for the mass of the nucleon – from ref. [5]. The two parameter fit corresponds to using eq. (4) with  $\gamma$  set equal to the value known from  $\chi$ PT. The three parameter fit corresponds to letting  $\gamma$  vary as an unconstrained fit parameter. The solid line is the two parameter fit based on the functional form of eq. (5).

with  $\alpha, \beta$  and  $\gamma$  fitted to the data. While this gives a very good fit to the data, the chiral coefficient  $\gamma$  is only  $-0.761$ , compared with the value  $-5.60$  required by chiral symmetry. If one insists that  $\gamma$  be consistent with QCD the best fit one can obtain with this form is the dash-dot curve. This is clearly unacceptable.

An alternative suggested recently by Leinweber *et al* [5], which also involves just three parameters, is to evaluate  $\sigma_{NN}$  and  $\sigma_{N\Delta}$  with the same ultra-violet form factor, with mass parameter  $\Lambda$ , and to fit  $M_N$  as

$$M_N = \alpha + \beta m_\pi^2 + \sigma_{NN}(m_\pi, \Lambda) + \sigma_{N\Delta}(m_\pi, \Lambda). \quad (5)$$

Using a sharp cut-off ( $u(k) = \theta(\Lambda - k)$ ) these authors were able to obtain analytic expressions for  $\sigma_{NN}$  and  $\sigma_{N\Delta}$  which reveal the correct LNA behaviour – and next to leading (NLNA) in the  $\Delta\pi$  case,  $\sigma_{N\Delta}^{\text{NLNA}} \sim m_\pi^4 \ln m_\pi$ . These expressions also reveal a branch point at  $m_\pi = M_\Delta - M_N$ , which is important if one is extrapolating from large values of  $m_\pi$  to the physical value. The solid curve in figure 1 is a two parameter fit to the lattice data using eq. (5), but fixing  $\Lambda$  at a value suggested by CBM simulations to be equivalent to the preferred 1 GeV dipole. A small increase in  $\Lambda$  is necessary to fit the lowest mass data point, at  $m_\pi^2 \sim 0.1 \text{ GeV}^2$ , but clearly one can describe the data very well while preserving the exact LNA and NLNA behaviour of QCD.

## 2.2 Consequences for the sigma commutator

The analysis of the lattice data for  $M_N$ , incorporating the correct non-analytic behaviour, can yield interesting new information concerning the sigma commutator of the nucleon:

$$\sigma_N = \frac{1}{3} \langle N | [Q_{i5}, [Q_{i5}, H_{\text{QCD}}]] | N \rangle = \langle N | \bar{m}(\bar{u}u + \bar{d}d) | N \rangle. \quad (6)$$

This is a direct measure of chiral SU(2) symmetry breaking in QCD, and the widely accepted experimental value is  $45 \pm 8 \text{ MeV}$  [6]. (Although there are recent suggestions that it might be as much as 20 MeV larger [7].) Using the Feynman–Hellmann theorem one can also write

$$\sigma_N = \bar{m} \frac{\partial M_N}{\partial \bar{m}} = m_\pi^2 \frac{\partial M_N}{\partial m_\pi^2}. \quad (7)$$

Historically, lattice calculations have evaluated  $\langle N | (\bar{u}u + \bar{d}d) | N \rangle$  at large quark mass and extrapolated this scale dependent quantity to the ‘physical’ quark mass, which had to be determined in a separate calculation. The latest result with dynamical fermions,  $\sigma_N = 18 \pm 5 \text{ MeV}$  [8], illustrates how difficult this procedure is. On the other hand, if one has a fit to  $M_N$  as a function of  $m_\pi$  which is consistent with chiral symmetry, one can evaluate  $\sigma_N$  directly using eq. (7). Using eq. (5) with a sharp cut-off yields  $\sigma_N \sim 55 \text{ MeV}$ , while a dipole form gives  $\sigma_N \sim 45 \text{ MeV}$  [9]. The residual model dependence can only be removed by more accurate lattice data at low  $m_\pi^2$ . Nevertheless, the result  $\sigma_N \in (45, 55) \text{ MeV}$  is in very good agreement with the data. In contrast, the simple cubic fit, with  $\gamma$  inconsistent with chiral constraints, gives  $\sim 30 \text{ MeV}$ . Until the experimental situation regarding  $\sigma_N$  improves, it is not possible to draw definite conclusions regarding the strangeness content of the nucleon. However, the fact that two-flavour QCD reproduces the current preferred value should certainly stimulate some thought and a lot of work.

### 3. Electromagnetic form factors

It is a general consequence of quantum mechanics that the long-range charge structure of the proton comes from its  $\pi^+$  cloud ( $p \rightarrow n\pi^+$ ), while for the neutron it comes from its  $\pi^-$  cloud ( $n \rightarrow p\pi^-$ ). However, it is not often realized that the LNA contribution to the nucleon charge radius goes like  $\ln m_\pi$  and diverges as  $\bar{m} \rightarrow 0$  [11]. This cannot be reproduced by a constituent quark model. Figure 2 shows the latest data from Mainz and NIKHEF for the neutron electric form factor, in comparison with CBM calculations for a confinement radius between 0.9 and 1.0 fm. The long-range  $\pi^-$  tail of the neutron plays a crucial role.

While there are only limited (and indeed quite old) lattice data for hadron charge radii, recent experimental progress in the determination of hyperon charge radii has led us to examine the extrapolation procedure for obtaining charge data from the lattice simulations [12]. Figure 3 shows the extrapolation of the lattice data [13] for the charge radius of the proton. Clearly the agreement with experiment is much better once the chiral log required by chiral symmetry is correctly included, than if, for example, one simply made a linear extrapolation in the quark mass (or  $m_\pi^2$ ). Full details of the results for all the octet baryons may be found in ref. [12].

The situation for baryon magnetic moments is also very interesting. The LNA contribution in this case arises from the diagram where the photon couples to the pion loop. As this involves two pion propagators the expansion of the proton and neutron moments is

$$\mu^{p(n)} = \mu_0^{p(n)} \mp \alpha m_\pi + \mathcal{O}(m_\pi^2). \quad (8)$$

Here  $\mu_0^{p(n)}$  is the value in the chiral limit and the linear term in  $m_\pi$  is proportional to  $\bar{m}^{\frac{1}{2}}$ , a branch point at  $\bar{m} = 0$ . The coefficient of the LNA term is  $\alpha = 4.4\mu_N \text{ GeV}^{-1}$ . At the

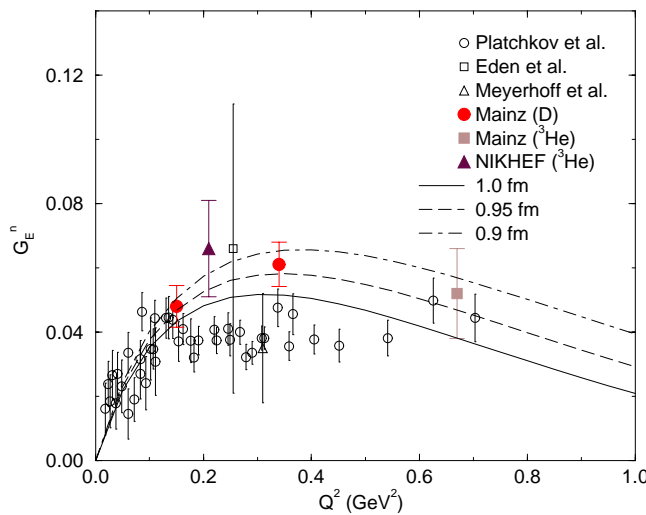


**Figure 2.** Recent data for the neutron electric form factor in comparison with CBM calculations for a confining radius around 0.95 fm – from ref. [10].

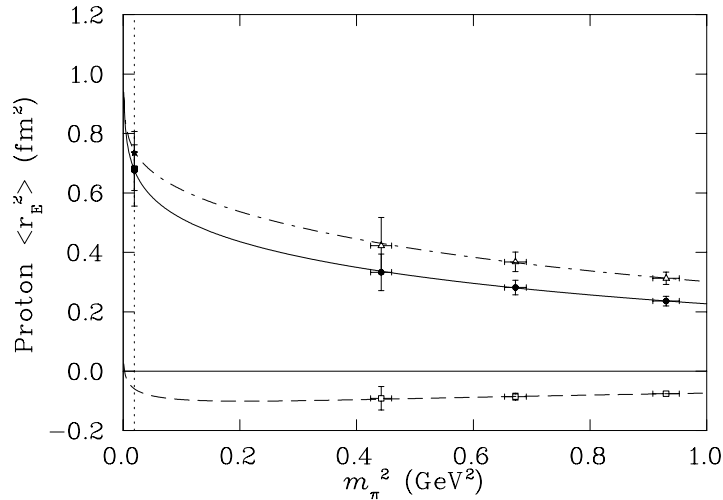


**Figure 3.** Fits to lattice results for the squared electric charge radius of the proton – from [12]. Fits to the contributions from individual quark flavours are also shown: the *u*-quark sector results are indicated by open triangles and the *d*-quark sector results by open squares. Physical values predicted by the fits are indicated at the physical pion mass, where the full circle denotes the result predicted from the first extrapolation procedure and the full square denotes the baryon radius reconstructed from the individual quark flavor extrapolations. (N.B. The latter values are actually so close as to be indistinguishable on the graph.) The experimental value is denoted by an asterisk.

physical pion mass this LNA contribution is  $0.6\mu_N$ , which is almost a third of the neutron magnetic moment. *No constituent quark model can or should get better agreement with data than this.*

Just as for  $M_N$ , the chiral behaviour of  $\mu^{p(n)}$  is vital to a correct extrapolation of lattice data. One can obtain a very satisfactory fit to some rather old data, which happens to be the best available, using the simple Padé [14]:

$$\mu^{p(n)} = \frac{\mu_0^{p(n)}}{1 \pm \frac{\alpha}{\mu_0^{p(n)}} m_\pi + \beta m_\pi^2}. \quad (9)$$

The data can only determine two parameters and eq. (9) has just two free parameters while guaranteeing the correct LNA behaviour as  $m_\pi \rightarrow 0$  and the correct behaviour of heavy quark effective theory (HQET) at large  $m_\pi^2$ . The extrapolated values of  $\mu^p$  and  $\mu^n$  at the physical pion mass,  $2.85 \pm 0.22\mu_N$  and  $-1.90 \pm 0.15\mu_N$ , respectively, are currently the best estimates from non-perturbative QCD [14]. For more details of this fit we refer to [14], while for the application of similar ideas to other members of the nucleon octet we refer to [15], and for the strangeness magnetic moment of the nucleon we refer to [16].

Incidentally, from the point of view of the naive quark model it is interesting to plot the ratio of the absolute values of the proton and neutron magnetic moments as a function of  $m_\pi^2$ . The agreement of the constituent quark result, namely  $3/2$ , with the experimental value to within a few percent is usually taken as a major success. However, we see

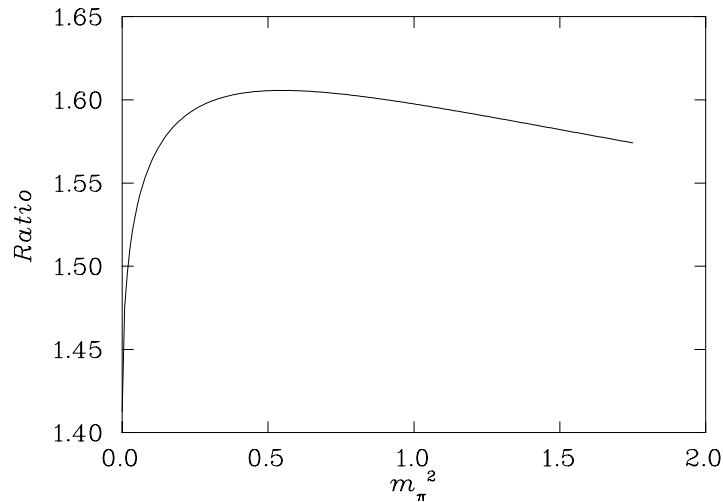


**Figure 4.** Absolute value of the ratio of the proton to neutron magnetic moments as a function of  $m_\pi^2$  obtained from the Padé approximants in eq. (9). We stress that the behaviour as  $m_\pi^2 \rightarrow 0$  is *model independent*.

from figure 4 that it is in fact fortunate to obtain such close agreement [17]. We stress that the large slope of the ratio near  $m_\pi^2 = 0$  is *model independent*.

#### 4. Structure functions

The parton distribution functions (PDFs) of the nucleon are light-cone correlation functions which, in the infinite momentum frame, are interpreted as probability distributions for finding specific partons (quarks, antiquarks, gluons) in the nucleon. They have been measured in a variety of high energy processes, ranging from deep-inelastic lepton scattering to Drell–Yan and massive vector boson production in hadron–hadron collisions. A wealth of experimental information now exists on spin-averaged PDFs, and an increasing amount of data is being accumulated on spin-dependent PDFs [18].

At high momentum transfer ( $Q^2$ ) the dominant component of the PDFs are determined by non-perturbative matrix elements of certain ‘leading twist’ operators. In principle these matrix elements, which correspond to moments of the measured structure functions, contain vital information about the non-perturbative structure of the target. An extensive phenomenology has been developed over the years within model QCD studies, and in some cases remarkable predictions have been made from the insight gained into the non-perturbative structure of the nucleon. An example is the  $\bar{d} - \bar{u}$  asymmetry, predicted [19] on the basis of the nucleon’s pion cloud [20], which has been spectacularly confirmed in recent experiments at CERN and Fermilab [21]. Other predictions, such as asymmetries between strange and antistrange [22] and spin-dependent sea quark distributions,  $\Delta\bar{u} - \Delta\bar{d}$ , still await experimental confirmation. Note that none of these could be anticipated without insight into the non-perturbative structure of QCD.

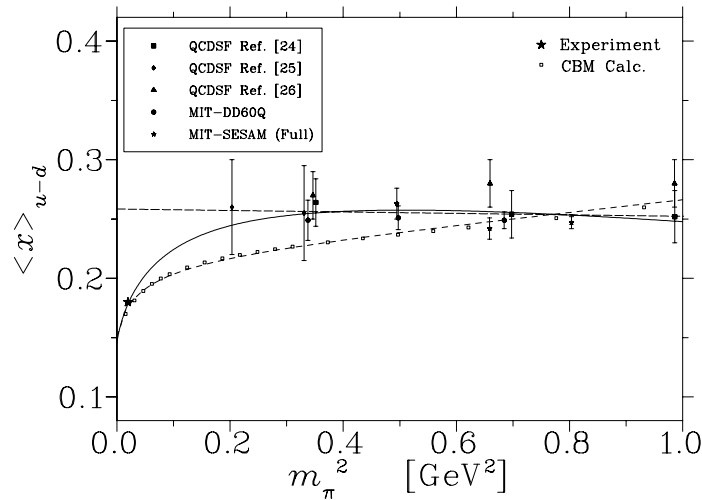


**Figure 5.** First moment of the difference  $u - d$  from various lattice QCD simulations (QCDSF [24–26] and MIT [27]), at a scale  $Q^2 = 4 \text{ GeV}^2$ . Calculations from the CBM are shown as small squares. The dashed curve is a simple fit which is linear in  $m_\pi^2$ , while the solid curve incorporates the constraints of chiral symmetry, as in eq. (10).

Despite the phenomenological successes in correlating deep-inelastic and other high energy data with low energy hadron structure, the *ad hoc* nature of some of the assumptions made in deriving the low energy models from QCD leaves open a number of questions about the ability to reliably assign systematic errors to the model predictions. One approach in which structure functions can be calculated systematically from first principles, and which at the same time allows one to search for and identify the relevant low energy QCD degrees of freedom, is lattice QCD.

Early calculations of structure function moments within lattice QCD were performed by Martinelli and Sachrajda [23]. However, the most comprehensive analysis has been performed by the QCDSF Collaboration [24–26] – albeit within quenched QCD. Recently the MIT group has performed the first full (unquenched) QCD calculations of non-singlet moments [27]. The moments from the full QCD simulations are very similar to those from the quenched calculations. This is consistent with the suggestions of chiral quark models, like the CBM, that in the mass region currently accessible quark loops are suppressed.

As for the other nucleon properties discussed above, we propose to extrapolate the lattice data to the physical pion mass using a formula which is compatible with the LNA structure of the PDFs. This behaviour was derived recently, with the result that the LNA behaviour involved a term in  $m_\pi^2 \ln m_\pi$  [28]. For an initial investigation we concentrate on the non-singlet combination of PDFs,  $u - d$ , in which ‘disconnected’ quark loops cancel. Calculations based on the CBM (which incorporate the LNA chiral structure just discussed) actually produce quite a reasonable description of the behaviour of the moments of the PDFs as a function of quark mass, as shown in figure 5 (open squares). More important from the phenomenological point of view, the CBM calculations (for the  $n$ th moment of the PDFs) can be fit with the simple expansion in  $m_\pi$ :

$$\langle x_u^n - x_d^n \rangle = a_n + b_n m_\pi^2 + a_n c_{\text{LNA}} m_\pi^2 \ln \left( \frac{m_\pi^2}{m_\pi^2 + \mu^2} \right), \quad (10)$$

where  $c_{\text{LNA}}$  is model independent.

The scale  $\mu$  in eq. (10) is effectively the scale at which the rapid, chiral variation at low  $m_\pi$  turns off. The best fit to the lattice data is obtained with a value  $\mu \sim 0.4\text{--}0.5$  GeV – a very similar scale to that found, for example, for the magnetic moments. Clearly eq. (10) gives a very good description of the lattice data for the first moment of the non-singlet distribution  $d - u$ . Taking into account the rapid chiral variation as  $m_\pi^2 \rightarrow 0$  there is also quite good agreement between the extrapolated value of the first moment and the experimentally determined moment. A similar result holds for the second and third moments too [29].

## 5. Conclusion

In the light of the numerous examples presented in this brief review, it should be evident that the study of hadron properties as a function of quark mass shows a clear pattern:

- In the region of quark masses  $\bar{m} > 60$  MeV or so ( $m_\pi$  greater than typically 400–500 MeV) hadron properties are smooth, slowly varying functions of something like a constituent quark mass,  $M \sim M_0 + c\bar{m}$  (with  $c \sim 1$ ).
- Indeed,  $M_N \sim 3M$ ,  $M_{\rho,\omega} \sim 2M$  and magnetic moments behave like  $1/M$ .
- As  $\bar{m}$  decreases below 60 MeV or so, chiral symmetry leads to rapid, non-analytic variation, with  $\delta M_N \sim \bar{m}^{3/2}$ ,  $\delta \mu_H \sim \bar{m}^{1/2}$  and  $\delta \langle r^2 \rangle_{\text{ch}} \sim \ln \bar{m}$ .
- Chiral quark models like the cloudy bag provide a natural explanation of this transition. The scale is basically set by the inverse size of the pion source – the inverse of the bag radius in the bag model.

These are remarkable results that will have profound consequences for our further exploration of hadron structure within QCD as well as the analysis of the vast amount of data now being taken concerning unstable resonances. In terms of immediate results for the structure of the nucleon, we note that the careful incorporation of the correct chiral behaviour of QCD into the extrapolation of its properties calculated on the lattice has produced:

- The best values of the proton and neutron magnetic moments from QCD.
- The best value of the sigma commutator.
- Improved values for the charge radii of the baryon octet.
- Improved values for the magnetic moments of the hyperons.
- Good agreement between the extrapolated moments of the non-singlet distribution  $u - d$  and the experimentally measured moments.

In addition, although we did not have time to discuss it, this approach has led to the best current value for the strangeness magnetic moment of the proton from lattice QCD,  $G_M^s = -0.16 \pm 0.18 \mu_N$  [16].

Clearly, while much has been achieved, even more remains to be done. It is vital that lattice calculations with dynamical fermions are pushed to the lowest possible quark masses,

taking advantage of developments of improved actions and so on. It is also vital to further develop our understanding of the physics of chiral extrapolation by comparison with these new calculations, by looking at new applications and by further comparison with chiral models.

### Acknowledgements

We would like to thank E Hackett-Jones, J Negele, K Tsushima, A Williams and R Young for helpful discussions of the matters discussed here. This work was supported by the Australian Research Council and the University of Adelaide and was presented by A W Thomas at the International Symposium on Nuclear Physics, Mumbai.

### References

- [1] T D Cohen, hep-ph/9512275
- [2] H Pagels, *Phys. Rep.* **16**, 219 (1975)
- [3] S Theberge, A W Thomas and G A Miller, *Phys. Rev.* **D22**, 2838 (1980)  
A W Thomas, *Adv. Nucl. Phys.* **13**, 1 (1984)
- [4] S Aoki et al, *Phys. Rev.* **D60**, 114508 (1999) [CP-PACS]  
C R Allton et al, *Phys. Rev.* **D60**, 034507 (1999) [UKQCD]
- [5] D B Leinweber et al, *Phys. Rev.* **D61**, 074502 (2000); hep-lat/9906027
- [6] J Gasser, H Leutwyler and M E Sainio, *Phys. Lett.* **B253**, 252 (1991)
- [7] M Knecht, hep-ph/9912443
- [8] SESAM Collaboration: S Gusken et al, *Phys. Rev.* **D59**, 054504 (1999)
- [9] D B Leinweber et al, *Phys. Lett.* **B482**, 109 (2000); hep-lat/0001007
- [10] D H Lu et al, in *Proc. Int. Conf. Few Body Problems* (Taipei, 2000), to appear in *Nucl. Phys.*  
D H Lu et al, *Phys. Rev.* **C60**, 068201 (1999); nucl-th/9807074
- [11] D B Leinweber and T D Cohen, *Phys. Rev.* **D47**, 2147 (1993); hep-lat/9211058
- [12] E J Hackett-Jones, D B Leinweber and A W Thomas, *Phys. Lett.* **B494**, 89 (2000); hep-lat/0008018
- [13] D B Leinweber, R M Woloshyn and T Draper, *Phys. Rev.* **D43**, 1659 (1991)
- [14] D B Leinweber et al, *Phys. Rev.* **D60**, 034014 (1999); hep-lat/9810005
- [15] E J Hackett-Jones, D B Leinweber and A W Thomas, *Phys. Lett.* **B489**, 143 (2000); hep-lat/0004006
- [16] D B Leinweber and A W Thomas, *Phys. Rev.* **D62**, 074505 (2000); hep-lat/9912052
- [17] D B Leinweber, A W Thomas and R D Young, hep-ph/0101211
- [18] M Erdmann, Talk given at *8th International Workshop on Deep Inelastic Scattering and QCD (DIS 2000)*, Liverpool, England, 25–30 Apr. 2000, hep-ex/0009009  
E W Hughes and R Voss, *Ann. Rev. Nucl. Part. Sci.* **49**, 303 (1999)
- [19] A W Thomas, *Phys. Lett.* **B126**, 97 (1983)
- [20] E M Henley and G A Miller, *Phys. Lett.* **B251**, 453 (1990)  
A I Signal, A W Schreiber and A W Thomas, *Mod. Phys. Lett.* **A6**, 271 (1991)  
W Melnitchouk, A W Thomas and A I Signal, *Z. Phys.* **A340**, 85 (1991)  
S Kumano, *Phys. Rev.* **D43**, 3067 (1991)  
S Kumano and J T Londergan, *Phys. Rev.* **D44**, 717 (1991)  
W-Y P Hwang, J Speth and G E Brown, *Z. Phys.* **A339**, 383 (1991)
- [21] P Amaudraz et al, *Phys. Rev. Lett.* **66**, 2712 (1991)

- A Baldit *et al*, *Phys. Lett.* **B332**, 244 (1994)  
E A Hawker *et al*, *Phys. Rev. Lett.* **80**, 3715 (1998)  
[22] A I Signal and A W Thomas, *Phys. Lett.* **B191**, 206 (1987)  
X Ji and J Tang, *Phys. Lett.* **B362**, 182 (1995)  
S J Brodsky and B-Q Ma, *Phys. Lett.* **B381**, 317 (1996)  
W Melnitchouk and M Malheiro, *Phys. Rev.* **C55**, 431 (1997)  
[23] G Martinelli and C T Sachrajda, *Phys. Lett.* **B196**, 184 (1987); *Nucl. Phys.* **B306**, 865 (1988)  
[24] M Göckeler, R Horsley, E M Ilgenfritz, H Perlt, P Rakow, G Schierholz and A Schiller, *Phys. Rev.* **D53**, 2317 (1996)  
[25] M Göckeler, R Horsley, E M Ilgenfritz, H Perlt, P Rakow, G Schierholz and A Schiller, *Nucl. Phys. Proc. Suppl.* **53**, 81 (1997)  
[26] C Best *et al*, hep-ph/9706502  
[27] D Dolgov *et al*, hep-lat/0011010  
[28] A W Thomas, W Melnitchouk and F M Steffens, *Phys. Rev. Lett.* **85**, 2892 (2000)  
[29] W Detmold *et al*, to be published